

COMMUNICATIONS

Resolution Enhancement and Spectral Editing of Uniformly ^{13}C -Enriched Proteins by Homonuclear Broadband ^{13}C Decoupling

GEERTEN W. VUISTER AND AD BAX

*Laboratory of Chemical Physics, National Institutes of Diabetes and Digestive and Kidney Diseases,
National Institutes of Health, Bethesda, Maryland 20892*

Received February 4, 1992

A number of heteronuclear 3D and 4D NMR techniques, developed in the past few years, make it possible to determine complete ^1H , ^{13}C , and ^{15}N resonance assignments for proteins of up to several hundred amino acids (1). Many of the experiments used in this assignment process rely on magnetization transfer via ^{13}C - ^1H , ^{13}C - ^{13}C , ^{13}C - ^{15}N , and ^{15}N - ^1H J couplings and for optimal sensitivity require a high level (typically >95%) of isotopic enrichment with ^{13}C and ^{15}N . Consequently, the ^1H -decoupled ^{13}C spectrum of such a protein exhibits ^{13}C resonances that are split by both heteronuclear ^{13}C - ^{15}N and homonuclear ^{13}C - ^{13}C J couplings, dramatically decreasing the spectral resolution. On spectrometers equipped for triple resonance, the effect of ^{13}C - ^{15}N J coupling can be removed in a straightforward manner by the use of broadband ^{15}N decoupling. Removal of the homonuclear ^{13}C - ^{13}C multiplet splitting cannot be obtained by the use of such a "brute force" method. Here we demonstrate that high resolution in the ^{13}C spectrum can be obtained in an efficient manner by using a "constant-time" ^{13}C evolution period. This approach, originally used for the same purpose in ^1H NMR (2, 3), has recently also been employed in a variety of heteronuclear 3D triple-resonance experiments (4-7). However, none of these 3D experiments exploited the very high resolving power obtainable in the ^{13}C dimension. The uniformity of one-bond aliphatic ^{13}C - ^{13}C J couplings makes it possible to optimize the constant-time ^{13}C evolution experiments in a straightforward manner, offering high resolution at a minimal cost in sensitivity and, as will be shown, providing information on the number of aliphatic carbons attached to a given ^{13}C .

Homonuclear ^{13}C decoupling by means of constant-time evolution is most easily implemented in experiments where the ^{13}C spins evolve as single-quantum coherence. We illustrate the use of this decoupling for correlating ^1H and ^{13}C chemical shifts by means of the heteronuclear single-quantum coherence (HSQC) technique, also known as the Overbodenhausen experiment (8, 9). However, the same advantages and disadvantages of constant-time ^{13}C evolution, discussed below for the HSQC experiment, also apply to a large variety of other pulse schemes.

The pulse scheme of the conventional HSQC experiment previously has been described in terms of the product-operator formalism (9). The constant-time HSQC (CT-HSQC) experiment, sketched in Fig. 1, differs from the conventional HSQC

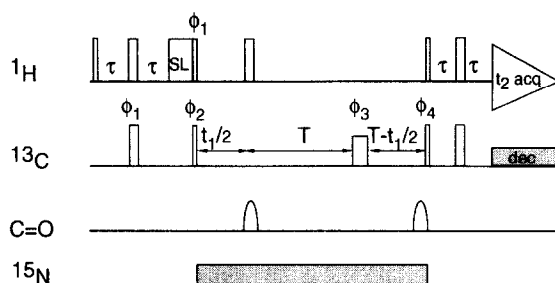


FIG. 1. Pulse scheme of the CT-HSQC experiment. Narrow and wide pulses denote 90° and 180° flip angles, respectively. All carbon pulses, with exception of the 180_{ϕ_3} refocusing pulse and the shaped carbonyl pulses, are high power. Power of the ^{13}C 180° refocusing pulse was adjusted in such a way that it causes zero excitation in the carbonyl region. Carbonyl 180° decoupling pulses are applied 20.0 kHz downfield from the ^{13}C carrier and implemented as phase-modulated pulses with an amplitude profile corresponding to the center lobe of a sinc function. The second shaped 180° carbonyl pulse, prior to the reverse INEPT sequence, refocuses ^{13}C evolution caused by the off-resonance effects of the first 180° carbonyl pulse [Bloch-Siegert effect (10)]. SL denotes a spin-lock pulse to suppress the residual HDO resonance (20). Unless indicated otherwise, all pulses are applied along the x axis. The minimum phase cycle resulting in artifact-free spectra is as follows: $\phi_1 = y, -y$; $\phi_2 = x$; $\phi_3 = 2(y), 2(-y), 2(-x), 2(x)$; $\phi_4 = 8(x), 8(-x)$; receiver = $2(x, -x), 4(-x, x), 2(x, -x)$. Quadrature detection in t_1 is obtained by the States-TPPI technique incrementing phase ϕ_2 (23). The delay τ was set to 1.7 ms. The constant time $2T$ of the experiment was set to either 26.6 or 53.2 ms, resulting in optimal refocusing for carbon-carbon couplings of 37.6 Hz. ^{13}C decoupling during ^1H data acquisition was accomplished with a synchronous ^{13}C GARP decoupling scheme (21), using an RF field strength of 4.5 kHz. ^{15}N decoupling during the constant-time evolution period was accomplished with an asynchronous WALTZ-16 decoupling scheme (22), using an RF field strength of 1.5 kHz.

method only in the way that ^{13}C transverse magnetization evolves during the period between the INEPT and the reverse INEPT transfers. Evolution of this transverse ^{13}C magnetization caused by heteronuclear ^{13}C - ^1H coupling, ^{13}C chemical-shift evolution, ^{13}C - ^{13}CO coupling, and aliphatic ^{13}C - ^{13}C couplings will briefly be discussed below. From Fig. 1 it can be readily seen that the heteronuclear coupling evolves for a period A :

$$A = t_1/2 - T + (T - t_1/2) = 0. \quad [1]$$

The ^{13}C chemical shift evolves for a period B :

$$B = t_1/2 + T - (T - t_1/2) = t_1. \quad [2]$$

The effect of J coupling between aliphatic and carbonyl carbons during the initial t_1 fraction of the constant-time evolution period is removed by the selective 180° CO pulse. During the remaining fraction of the constant-time evolution period, dephasing caused by this coupling is eliminated by the 80_{ϕ_3} pulse applied to the aliphatic carbons. The selective 80° CO pulse applied at the end of the constant-time evolution period merely serves to negate the phase error caused by the Bloch-Siegert shift (10) present during the first 180° CO pulse. Finally, the effect of aliphatic ^{13}C - ^{13}C couplings, not affected by the 80_{ϕ_3} pulse, evolves for a period C :

$$C = t_1/2 + T + (T - t_1/2) = 2T. \quad [3]$$

Aliphatic one-bond ^{13}C – ^{13}C J couplings typically fall in the 32–40 Hz range and will be denoted by a single value J_{CC} . Evolution of transverse magnetization, S_{1x} , of an aliphatic carbon, caused by one-bond ^{13}C – ^{13}C couplings to n other aliphatic carbons, yields

$$S_{1x} \rightarrow S_{1x} \cos^n(2\pi J_{\text{CC}}T) + \dots, \quad [4]$$

where \dots denotes antiphase ^{13}C magnetization terms of the form S_{1y} , S_{2z} and $S_{1x}S_{2z}S_{3z}$, which are not converted back to observable proton magnetization by the reverse INEPT at the end of the period, $2T$. Consequently, if the constant-time $2T$ is adjusted to a multiple of $1/J_{\text{CC}}$, the ^{13}C magnetization is in phase with respect to its directly coupled ^{13}C nuclei at the end of the period $2T$, independent of the duration of t_1 (Eq. [4]). Therefore, ^{13}C magnetization at the end of the constant-time evolution period is modulated only by its chemical-shift frequency, and correlations in the 2D spectrum will appear as singlets in the ^{13}C dimension. As is seen from Eq. [4], if $2T$ is adjusted to $1/J_{\text{CC}}$ the sign of the ^{13}C magnetization is opposite for carbons coupled to an odd versus an even number of coupling partners, n . For example, all glycine $^{13}\text{C}_\alpha$ cross peaks have opposite sign to all other C_α correlations since the first are not coupled to any other aliphatic ^{13}C spins. If, however, the delay $2T$ is tuned to $2/J_{\text{CC}}$ all peaks will have the same sign.

Before the technique is illustrated, one experimental detail requires additional explanation. In the discussion given above, J coupling to carbonyl nuclei was removed by a selective 180° pulse and by using a $180^\circ_{\phi_3}$ pulse with a null in its excitation profile at the carbonyl frequency. This latter requirement restricts the RF power that can be used for this pulse and causes imperfect inversion of ^{13}C nuclei that resonate near the edges of the aliphatic region of the ^{13}C spectrum. As a consequence, a small fraction of the transverse magnetization from a ^{13}C coupled to such a poorly inverted ^{13}C spin will not be decoupled and will give rise to a doublet structure superimposed on the parent decoupled ^{13}C resonance. For the case where $2T = 1/J_{\text{CC}}$, this spurious doublet is antiphase with respect to the decoupled resonance and actually gives the latter the appearance of a resolution-enhanced lineshape. For $2T = 2/J_{\text{CC}}$, the spurious doublet is in phase with respect to the decoupled center resonance, giving it the appearance of a triplet with an intense central component and a splitting of J_{CC} between the outer components. Artifacts of a similar nature previously have been described for the classic proton-flip experiment (11), and as was argued for that case, they cannot be removed by phase cycling. Instead, to reduce the artifact in the present CT-HSQC experiment, the $180^\circ_{\phi_3}$ can be applied at high RF power. In the latter case, artifacts appear for ^{13}C nuclei that are coupled to carbonyl spins, but the intensity of the spurious doublets mentioned above is reduced for the remaining ^{13}C resonances.

The method is demonstrated for a 1.0 mM solution of the protein calmodulin (M_r 16.7 kDa), uniformly enriched (>95%) with ^{13}C and ^{15}N and complexed with four molar equivalents of Ca^{2+} , dissolved in D_2O , pH 6.8. All experiments were recorded at 35°C on a Bruker AMX600 operating at a ^1H resonance frequency of 600.14 MHz. The results from the constant-time HSQC spectra, recorded with constant-time evolution periods ($2T$) of $1/J_{\text{CC}}$ and $2/J_{\text{CC}}$, are compared with the results obtained from the regular HSQC experiment.

All experiments were carried out with the ^{13}C transmitter positioned at 43 ppm and using a 90° pulse width of 14 μs . The $180^\circ_{\phi_3}$ pulse was applied either at a power level

corresponding to a $43 \mu\text{s}$ 180° pulse (yielding zero excitation at the carbonyls) or at the same power as the other ^{13}C pulses (i.e., with a $28 \mu\text{s}$ pulse width). For both the conventional HSQC experiment and for the CT-HSQC experiment where $2T$ was set to $1/J_{\text{CC}}$, $128 \text{ complex } (t_1) \times 384 \text{ complex } (t_2)$ data points were acquired, corresponding to acquisition times of $26.6 \text{ ms } (t_1)$ and $53.0 \text{ ms } (t_2)$. For the CT-HSQC experiment with $2T = 2/J_{\text{CC}}$, $256 \text{ complex } (t_1) \times 384 \text{ complex } (t_2)$ data points were acquired, corresponding to acquisition times of 53 ms in both dimensions. For each complex t_1 increment, 32 scans were recorded, resulting in 68 and 139 min measuring times for the smaller and the larger data matrix, respectively.

For all data sets, the t_2 time domain was zero-filled to 1024 complex points. After windowing (72° -shifted squared sine bell), Fourier transformation, and phasing in the F_2 dimension, the length of the t_1 time domain was doubled by mirror-image linear prediction (12) for the constant-time experiments and by normal linear prediction (13, 14) for the conventional HSQC data, followed by zero filling to 1024 complex points. After windowing (Gaussian multiplication) and Fourier transformation, this yielded a real data set of 1024×1024 points with a digital resolution of $4.8 \text{ Hz/point } (F_1)$ and $7.1 \text{ Hz/point } (F_2)$.

For the conventional HSQC experiment, the finite duration of the pulses results in a linear phase error in the F_1 domain of the spectrum. In order to minimize the baseline distortion resulting from the F_1 phase correction, the initial t_1 delay was set in such a way that a -90° zero-order and $+180^\circ$ first-order phase correction error was required (15). As a result, in the conventional HSQC spectrum all peaks that have folded once are of opposite sign to nonfolded peaks. In contrast, in the constant-time experiment where sampling starts at $t_1 = 0$, no linear phase correction in the F_1 domain is needed. Consequently, folded and nonfolded peaks are of identical sign.

Spectra obtained with the conventional HSQC technique and with the CT-HSQC scheme are compared in Fig. 2. The boxed regions of the spectrum are shown in more detail in Fig. 3. As can be seen from these spectra, the CT-HSQC spectra yield a dramatic increase in resolution over the conventional HSQC spectrum. Figures 3a–3c compare expanded plots of a region showing $\text{H}_\alpha\text{--C}_\alpha$ correlations of the three spectra. In this crowded region, several glutamates, lysines, and phenylalanines resonate. In the conventional HSQC spectrum, only three such correlations (for residues H107, F19, and F92) can be identified. In contrast, the CT-HSQC spectra permit identification of a large number of resonances in this crowded region of the spectrum. Resolution is particularly high in the CT-HSQC spectrum recorded with $2T = 53.2 \text{ ms}$ (Fig. 3c), although the difference in intensity caused by differences in the $^{13}\text{C}_\alpha$ transverse relaxation rates gives rise to significant intensity anomalies in this spectrum. To obtain this high resolution in the F_1 dimension it was necessary to use broadband ^{15}N decoupling during the constant-time evolution period, $2T$. The improvement in resolution obtained by the CT-HSQC experiment over the conventional HSQC experiment is dramatic. In fact, in the spectrum in Fig. 2c, 142 such correlations out of a maximum of 159 (148 residues including 11 glycines) are at least partially resolved.

Figures 3d–3f compare an expanded region containing correlations for the side-chain $\text{H}_\gamma\text{--C}_\gamma$ and $\text{H}_\beta\text{--C}_\beta$ correlations of methionine, glutamine, valine, and lysine residues. This region illustrates the editing capability of the CT-HSQC experiment: In the CT-HSQC spectrum with $2T = 1/J_{\text{CC}}$, the correlations to methionine C_γ are of opposite sign to the correlations involving lysine C_β carbons because Met- C_γ has

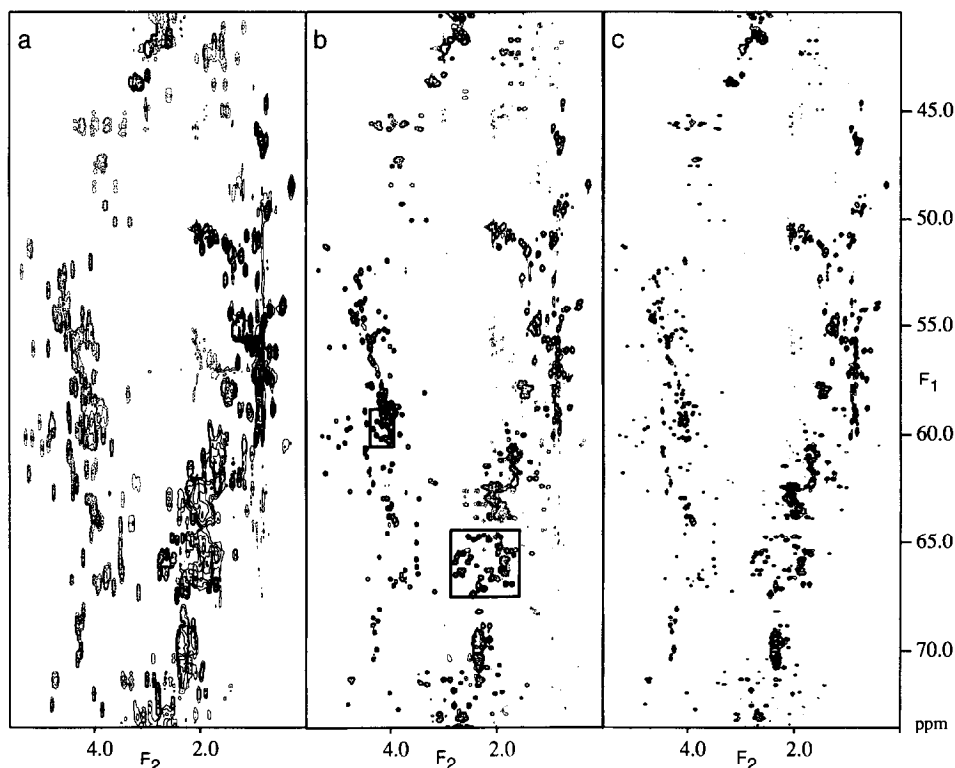
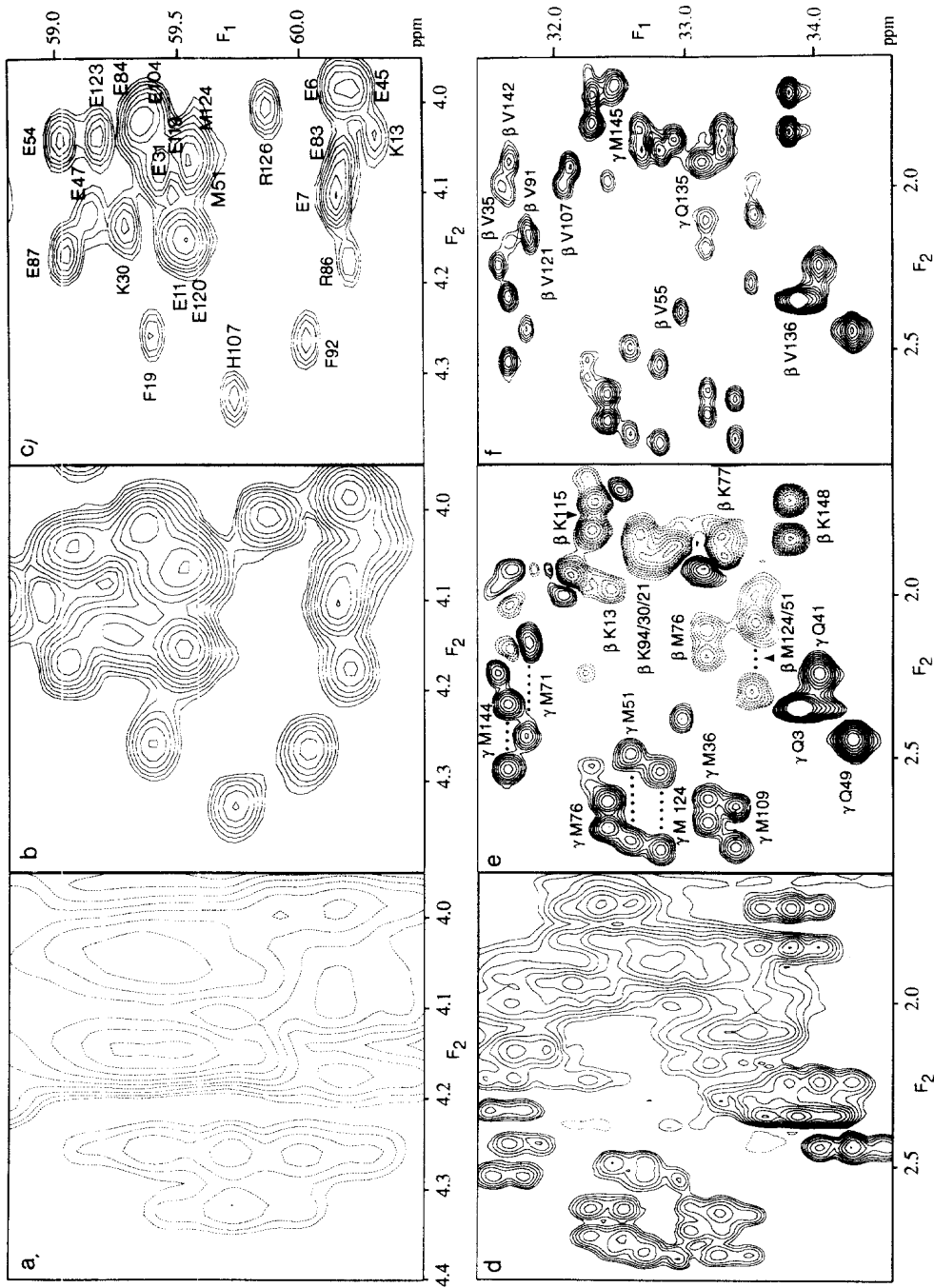


FIG. 2. Comparison of the ^1H - ^{13}C shift correlation spectra of the protein calmodulin recorded with (a) the regular HSQC experiment, (b) the CT-HSQC experiment with $2T = 26.6$ ms, and (c) the CT-HSQC experiment with $2T = 53.2$ ms. Details regarding the acquisition and processing of the spectra are given in the text. The spectral width in the ^{13}C dimension was adjusted to 5000 Hz (33 ppm) and the carrier was shifted postprocessing to 57 ppm. Therefore, resonances resonating upfield of 40.5 ppm appear at F_1 frequencies that are 33 ppm downfield from their actual chemical shift. Expansions of the three spectra for the regions boxed in (b) are shown in Fig. 3.

only a single ^{13}C coupling partner, whereas Lys- C_β has two. Note that this editing is different from editing based on the proton multiplicity, where the two types of CH_2 moieties would be indistinguishable.

Homonuclear decoupling by means of a constant-time evolution period works well only for weakly coupled spin systems (3). For the ^{13}C case, this requirement refers to the ^1H -coupled ^{13}C spectrum. For adjacent methylene carbons, for example, this means

FIG. 3. Expanded regions of the three spectra shown in Fig. 2. (a, d) Expansions of the spectrum in Fig. 2a, (b, e) expansions of the spectrum in Fig. 2b, and (c, f) expansions of the spectrum in Fig. 2c. Negative contour levels are shown as solid lines and positive levels as dashed contours. As discussed in the text, folded resonances in Fig. 2a [and (a) and (d) in the present figure] appear with negative intensity due to the 180° linear phase correction used in the F_1 dimension. For the CT-HSQC spectra, no phase correction was needed in the F_1 dimension, and negative contour levels correspond to carbons with an odd number of aliphatic carbon neighbors. Assignments are taken from Refs. (24, 25).



that the ^{13}C chemical shifts of the coupled ^{13}C nuclei must differ by more than $J_{\text{CC}} + 2^1 J_{\text{CH}}$. In practice, however, the artifacts introduced by strong ^{13}C - ^{13}C coupling tend to be quite weak for the aliphatic region of the spectrum. In contrast, for the aromatic ring carbons of the phenylalanine residues, which cluster in the 130–133 ppm region, artifacts introduced by strong ^{13}C - ^{13}C coupling seriously distort the spectrum.

The F_1 resolution of the CT-HSQC experiments is limited by the length of the constant-time evolution period, $2T$. The increase in resolution obtainable by changing $2T$ from 26 to 53 ms can be clearly seen in Fig. 3. The length of the maximum duration of $2T$ that can be used (i.e., the maximum F_1 resolution) is limited by several factors. First, ^{13}C T_2 relaxation during the time $2T$ attenuates the signal by $\exp(-2T/T_2)$. This attenuation can be very different for carbons with different T_2 values. For example, for the C_α carbons of the protein interferon- γ (31 kDa) intensity differences of nearly 100-fold were observed for the mobile versus the nonmobile carbons, even with a $2T$ period of only 26 ms (S. Grzesiek, unpublished results). Second, for $2T$ durations longer than 53 ms, variations in the size of the one-bond J_{CC} coupling make it impossible to optimize the experiment for the whole range of J_{CC} couplings simultaneously. Finally, for longer durations of $2T$, modulation caused by multiple-bond J_{CC} couplings can become significant and attenuate signal intensity. Therefore, in practice it is probably undesirable to use $2T$ durations longer than ~ 53 ms.

As mentioned earlier, the enhanced resolution available with the constant-time evolution period can be useful in a whole range of 3D and 4D experiments. Implementation is particularly straightforward in the ^{13}C separated NOE techniques (16, 17), where the HMQC step is to be replaced by the CT-HSQC method described above. As mentioned previously, a host of other 3D experiments can also easily incorporate the CT-HSQC building block (4–7, 18, 19). However, to obtain the maximum ^{13}C resolution in such experiments it is necessary to use a large number of t_1 increments in the ^{13}C dimension, which can result in measuring times for the 3D or 4D spectrum that cannot easily be accommodated in practice.

ACKNOWLEDGMENTS

We thank Guang Zhu for help with the linear prediction software. This work was supported by the AIDS Targeted Anti-Viral Program of the Office of the Director of the National Institutes of Health. G.W.V. acknowledges financial support from the Netherlands Organization of Scientific Research (NWO).

REFERENCES

1. G. M. CLORE AND A. M. GRONENBORN, *Prog. Nucl. Magn. Reson. Spectrosc.* **23**, 43 (1991).
2. A. BAX, A. F. MEHLKOPF, AND J. SMIDT, *J. Magn. Reson.* **35**, 373 (1979).
3. A. BAX AND R. FREEMAN, *J. Magn. Reson.* **44**, 542 (1981).
4. O. W. SØRENSEN, *J. Magn. Reson.* **90**, 433 (1990).
5. R. POWERS, A. M. GRONENBORN, G. M. CLORE, AND A. BAX, *J. Magn. Reson.* **94**, 209 (1991).
6. A. BAX AND M. IKURA, *J. Biomol. NMR* **1**, 99 (1991).
7. S. GRZESIEK AND A. BAX, *J. Magn. Reson.* **96**, 432 (1992).
8. G. BODENHAUSEN AND D. J. RUBEN, *Chem. Phys. Lett.* **69**, 185 (1980).
9. A. BAX, M. IKURA, L. E. KAY, D. A. TORCHIA, AND R. TSCHUDIN, *J. Magn. Reson.* **86**, 304 (1990).
10. R. FREEMAN, "A Handbook of Nuclear Magnetic Resonance," p. 14, Wiley, New York, 1988.
11. G. BODENHAUSEN AND D. L. TURNER, *J. Magn. Reson.* **41**, 200 (1980).

12. G. ZHU AND A. BAX, *J. Magn. Reson.* **90**, 405 (1990).
13. Y. ZENG, J. TANG, C. A. BUSH, AND J. R. NORRIS, *J. Magn. Reson.* **83**, 473 (1989).
14. E. T. OLEJNICZAK AND H. L. EATON, *J. Magn. Reson.* **87**, 628 (1990).
15. A. BAX, M. IKURA, L. E. KAY, AND G. ZHU, *J. Magn. Reson.* **91**, 174 (1991).
16. M. IKURA, L. E. KAY, R. TSCHUDIN, AND A. BAX, *J. Magn. Reson.* **86**, 204 (1990).
17. E. R. P. ZUIDERWEG, L. P. MCINTOSH, F. W. DAHLQUIST, AND S. W. FESIK, *J. Magn. Reson.* **86**, 210 (1990).
18. S. W. FESIK, H. L. EATON, E. T. OLEJNICZAK, E. R. P. ZUIDERWEG, L. P. MCINTOSH, AND F. W. DAHLQUIST, *J. Am. Chem. Soc.* **112**, 886 (1990).
19. A. BAX, G. M. CLORE, AND A. M. GRONENBORN, *J. Magn. Reson.* **88**, 425 (1990).
20. B. A. MESSERLE, G. WIDER, G. OTTING, C. WEBER, AND K. WÜTHRICH, *J. Magn. Reson.* **85**, 608 (1989).
21. A. J. SHAKA, P. BARKER, AND R. FREEMAN, *J. Magn. Reson.* **53**, 313 (1983).
22. A. J. SHAKA, J. KEELER, T. FRENKIEL, AND R. FREEMAN, *J. Magn. Reson.* **52**, 334 (1983).
23. D. MARION, M. IKURA, R. TSCHUDIN, AND A. BAX, *J. Magn. Reson.* **85**, 393 (1989).
24. M. IKURA, L. E. KAY, AND A. BAX, *Biochemistry* **29**, 4659 (1990).
25. M. IKURA, S. SPERA, G. BARBATO, L. E. KAY, M. KRINKS, AND A. BAX, *Biochemistry* **30**, 9216 (1991).